PCCP

Accepted Manuscript

ROYAL SOCIETY OF CHEMISTRY

www.rsc.org/pccp

ARTICLE TYPE www. rsc.org/xxxxxx | XXXXXXXX

A quasi-classical trajectory study of the OH + SO reaction: the role of ro-vibrational energy†

W. A. D. Pires,[a] J. D Garrido,[b‡] M. A. C. Nascimento,[b] and M. Y. Ballester [a*]

Received Xth XXXXXXXXXX 20XX, Accepted Xth XXXXXXXXX 20XX
First published on the web Xth XXXXXXXXXX 200X
DOI: 10.1039/b000000x

A study of the reaction $OH + SO \rightarrow H + SO_2$ using quasi-classical trajectory method is presented with the aim of investigating the role of the ro-vibrational energy of the reactants in the reactivity. The calculations were carried out using a previously reported global potential energy surface for $HSO_2(^2A)$. Different initial conditions with one and both reactants ro-vibrationally excited were studied. The reactive cross sections, for each studied combination, are calculated and then fitted to a capture-like model combined with a factor accounting for recrossing effects. The Vibrational Energy Quantum Mechanical Threshold of the Complex method was used to correct for the zero-point vibrational energy leakage of the classical calculations. State specific and averaged rate constants are reported. The reactivity is affected when ro-vibrational energy of any of both reactants is changed. The present calculations provides a theoretical support for the experimental rate constant for temperatures below 550 K, but fails to account for the significant fall in observed rate constant with increasing temperature above this value.

1 Introduction

Reactive collisions between hydroxyl radical and sulfur oxides are of interest in combustion and atmospheric chemistry[1,2]. Particularly, the reaction:

$$OH + SO \rightarrow H + SO_2 \quad (1)$$

has been extensively studied, both theoretically[3–11] and experimentally[12–14]. In previous works[10,11], details of the reaction mechanism were presented and using quasi-classical trajectories calculations and the double many body expansion (DMBE) potential energy surface described in Ref. 15, the effect of temperature and rotational energy on the reaction 1 was investigated. In such studies, the calculated rate constants were compared with the experimental data from the literature[12–14] and it was theoretically verified that the consideration of rotational excitation of the species OH and SO does not led to the sudden drop of the rate constant when the temperature rises above 500 K as Blitz *et al.* have reported[14]. Such observation led us to evaluate the role of ro-vibrational energy in the title reaction. Thus, the aim of this work is to study how the reactivity is affected when considering reactants rotationally and vibrationally excited using, for such a purpose, a global six-dimensional potential energy surface to describe the interactions of the molecular system, and quasi-classical trajectories methodology.

The paper is organized as follows. Salient features of the potential energy surface are presented in the next section, followed by a brief survey of the trajectory calculations methodology. Results of the calculations are discussed and compared with the literature in Section 4. Main conclusions are gathered in the last section.

2 Potential energy surface

To represent the inter-atomic interactions, a six-dimensional double many-body expansion (DMBE) potential energy surface (PES) for the ground electronic state of HSO_2 was used[15]. Such a surface employs DMBE functions previously reported for the diatomic and triatomic fragments and four-body energy terms to mimic *ab initio* CASPT2/FVCAS/AVXZ (X=2,3) calculations for the tetratomic system. The DMBE PES presents two paths, from the reactants $OH + SO$, to the only products, $H + SO_2$, allowed to be formed for the energy range studied in this work (Figure 1). Notice the absence of a barrier for reactants to produce intermediate species. The same nomenclature used before[15] is used in the present study. Thus, HOSO stands for the global minimum with the hydrogen atom bonded to oxygen, lying 71.8 kcal/mol below the $OH + SO$ limit; TS_1 (18.5 kcal/mol below $OH + SO$) denotes the transition state to form $H + SO_2$ directly from HOSO and the transition state TS_2 (18.2 kcal/mol above the TS_1) connects the HOSO global

† Electronic Supplementary Information (ESI) available. See DOI: 10.1039/b000000x/

[a] *Departamento de Física, Universidade Federal de Juiz de Fora-UFJF, Juiz de Fora, MG 36036-330, Brazil; E-mail: maikel.ballester@ufjf.edu.br*
[b] *Centro Interdisciplinar de Ciências da Natureza, Universidade Federal da Integração Latino-Americana-UNILA, Foz do Iguaçú, PR 85867-970, Brazil.*
[c] *Instituto de Química, Universidade Federal do Rio de Janeiro, RJ 21941-909, Brazil.*

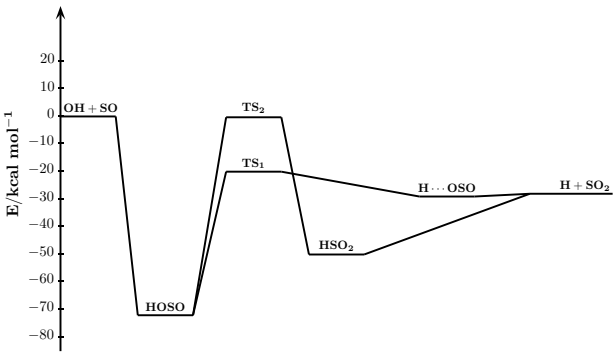

Fig. 1 Energy profile for the title reaction as obtained from the HSO_2 PES (Ref. 15).

minimum to the $H + SO_2$ limit through the HSO_2 isomer.

A salient feature of interest to the present work, is the predicted thermochemistry for reaction 1. Combining the enthalpy values reported by Wheeler and Schaefer III in an *ab initio* study on the HOSO radical[16], we obtain $\Delta H_{0K} = 29.4$ kcal mol^{-1}, while from the HSO_2 DMBE PES[15] we get $\Delta H = 30.17$ kcal mol^{-1} at 0 K, which reproduces very well the above mentioned *ab initio* results.

The HSO_2 DMBE PES was also used[17] in a quasi-classical trajectory study of the inverse reaction

$$H + SO_2 \rightarrow OH + SO, \tag{2}$$

and the rate constant values there obtained are in very good agreement with the experimental data. Recently Mc Carthy *et al.*, in a rotational spectroscopy study, reported angles and bond distances for the HOSO structure[18]. Values there presented concur with the corresponding geometry obtained from the DMBE PES. These results indicate that the DMBE PES is accurate and reliable for the purpose of this work. It is worth mentioning that recent works have reported discrepancies between high level *ab initio* calculations and the above mentioned DMBE PES[19,20], but the qualitative differences there reported refer to other regions of the PES which are not considered in this work.

3 Computational procedure

The quasi-classical trajectories (QCT) were obtained with the MERCURY program[21], using the HSO_2 DMBE potential energy surface. To assert the study of the role of vibrational energy, specific initial state calculations were carried out for selected vibrational-rotational quantum numbers of the reactants, heretofore referred as v_{SO},v_{OH},j_{SO} and j_{OH}. For all combinations, the initial translational energy covered the range $0.199 \leq E_{tr}/\text{kcal mol}^{-1} \leq 9.936$. For such calculations the molecules were kept at their respective rotational ground states, which means $j_{OH} = 1$ and $j_{SO} = 0$ assuming that OH follows Hund's rule case b)[22]. Nevertheless, to obtain vibrationally and rotationally averaged thermal rate coefficients (to be discussed later), two sets of rotational quantum numbers were also considered for selected vibrational combinations.

To run trajectories, the reactants were initially set at 10 Å appart, to make the interaction energy between them essentially negligible. The value of the time step used for the numerical integration was of 2.5×10^{-16}s, which warrants conservation of the total energy to better than one part in 10^3. The maximum impact parameter has been found by running batches of 100 trajectories at fixed values, with b_{max} being reduced until the reaction takes place. Such a procedure allows b_{max} to be determined within ± 0.1 Å. For the cases where only the OH radical is vibrationally excited and the translational energy is relatively small we obtained the same values previously reported for b_{max}[11].

Batches of 2000 trajectories were run for each combination of translational and vibrational energies. Such a number produces a reactive cross section with an error of typically a few percent ($\delta\sigma_R^{max} = 11.6\%$).

The reactive cross section is given by[23]

$$\sigma_R(E_{tr}; v_{OH}, j_{OH}, v_{SO}, j_{SO}) = \pi b_{max}^2 \frac{N_R}{N_T} \tag{3}$$

and the associated uncertainty is

$$\Delta\sigma_R = \left(\frac{N_T - N_R}{N_T N_R}\right)^{1/2} \sigma_R, \tag{4}$$

where N_R is the number of reactive trajectories in a total of N_T, N_R/N_T is the reaction probability(P_R). Assuming a Maxwell-Boltzmann distribution over the translational energy (E_{tr}), the specific rate coefficient is obtained as:

$$k(T; v_{OH}, j_{OH}, v_{SO}, j_{SO}) = g_e(T) \left(\frac{2}{k_B T}\right)^{3/2} \left(\frac{1}{\pi\mu}\right)^{1/2} \times$$
$$\times \int_0^\infty E_{tr} \sigma_R(E_{tr}; v_{OH}, j_{OH}, v_{SO}, j_{SO}) \exp\left(-\frac{E_{tr}}{k_B T}\right) dE_{tr} \tag{5}$$

where T is the temperature, μ is the reactants reduced mass, k_B is the Boltzmann constant and $g_e(T)$ is the electronic degeneracy factor, which assumes the form[10,24,25]:

$$g_e(T) = \frac{1}{3[1 + \exp(-205/T)]} \tag{6}$$

The zero point vibrational energy (ZPVE) leakage of the classical trajectories is a well known problem. Several methodologies have been proposed to deal with such a problem[26–28]. In this work we used the Vibrational Energy Quantum Mechanical Threshold of the Complex ($VEQMT_C$)[29] method. According to this procedure, only the trajectories for which the total

vibrational energy of the products exceeds their corresponding ZPEs are considered in the statistical analysis.

As before[10], we used a geometric criterion to define whether complex formation has occurred. According to such a criterion, complex formation is defined by means of two distances: one ensuring that the incoming hydroxyl radical is bonded to sulfur, the other checking whether the H atom is part of the four-body moiety or, instead, far away in the region of the products $H + SO_2$. A complex is then any arrangement of the four atoms $H - O_a - S - O_b$, such that the HS and SO_a distances become shorter than 1.3 times their values at the global minimum. Such a definition leads to complex lifetimes that agree well with those obtained from the distance vs time plots for randomly selected trajectories. Indeed, we find such a procedure to be sufficiently rigorous to avoid the cumbersome procedure of checking the bond distance vs time plots for all trajectories that have been run, although checks have been performed to warrant the accuracy of the method during mass production of the trajectory results.

The analysis of non-reactive trajectories (see later) requires a boxing procedure to assign the final vibrational energy E_f^x on each product molecule, where x stands for OH or SO which are the products for the recrossing trajectories. The method used in this work defines the energy gap associated with level $E_f^x(v)$ as:

$$\frac{E^x(v_i) - E^x(v_i - 1)}{2} < E_f^x(v) < \frac{E^x(v_i + 1) - E^x(v_i)}{2} \qquad (7)$$

where $E^x(v_i)$ are the energy values for the vibrational levels of OH and SO [the energy $E^x(-1)$ is defined to be zero]. Of course, the boxing procedure is always a source of error[30]. However, we used for comparison the specific initial-state deactivation probability (i.e. the probability of transition from the initial vibrational state corresponding to the energy E_i^x for the x species to any smaller final vibro-rotational energy E_f^x of deactivated molecule), instead of the state-to-state relaxation probability, which tends to minimize such errors in the assignment process[31]. The specific initial-state deactivation probability can be defined as:

$$P_{E_i}^{x\downarrow} = \sum_{E_f^x = E_0^x}^{E^x(v_i - 1)} P_{E_i, E_f^x}^{x\downarrow} \qquad (8)$$

where $P_{E_i,E_f^x}^{x\downarrow} = N_{E_i,E_f^x}^{x\downarrow}/N_T$ is the state-to-state deactivation probability.

4 Results and discussion

Table 1 collects the results for trajectory calculations when one or both reactants are vibrationally excited. For brevity, only trajectory results of three combinations of vibrational quantum numbers are shown. The full list of results is given as electronic supplementary information to this paper. In Table 1, as before[11], N_{com} is the number of trajectories forming a complex, while N_{rec} is the number of recrossing trajectories, i.e., those trajectories which break down the complex towards the reactants. These values were used to construct the Figure 2 showing how the reactive cross section is affected by the increase of vibrational energy. In all batches it was verified that $N_{com} = N_R + N_{rec}$. As before[11], no formation of HSO_2 was observed. Thus, all reactive trajectories evolves through the TS_1.

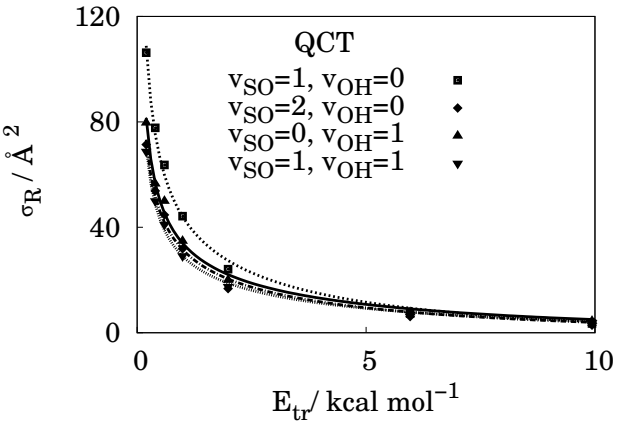

Fig. 2 Reactive cross section (σ_R) versus E_{tr} for the reaction $OH + SO \rightarrow H + SO_2$, with its respective functions fitted. Some selected vibrational combinations are shown.

Since the title reaction is exothermic the number of reactive trajectories is negligibly modified when the ZPVE is taken into account. However, the number of non-reactive trajectories, and consequently the total number of trajectories, can be significantly reduced. Thus, the $VEQMT_C$ method furnishes a higher value for the reactive cross section when compared to QCT. The studied reaction is barrier-less in our potential energy surface and it is dominated by long-range (mostly dipole-dipole) intermolecular interactions. It is known that the cross section for this kind of reactions decreases when translational energy increases[32,33] and this is exactly the behavior observed in Figure 2 for the cross section calculated in this work. As far as the influence of the degree of vibrational excitation is concerned, Figure 3 shows different variations in the reactive cross section depending on which reactant is vibrationally excited. From such a Figure, it is clear that when SO is the excited species the reactive cross section decreases with an increase on the vibrational energy and tends to a constant value for large vibrational energies. On the other hand, when OH is the excited species the reactive cross section first decreases for $v_{OH} = 1$, and then raises with further increase of vibrational energy. We also considered cases where both reactants

Table 1 Summary of trajectory calculations for selected ro-vibrational combinations of the reactants

v_{OH}, v_{SO}	E_{tr}/ kcal mol^{-1}	b_{max}/ Å	QCT				VEQMT$_C$			
			N_T	N_{com}	N_{rec}	N_r	N_T	N_{com}	N_{rec}	N_r
0,3	0.199	8.8	2000	1617	1128	489	1563	1192	714	478
	0.396	7.9	2000	1560	1132	428	1563	1127	703	424
	0.596	7.2	2000	1506	1067	439	1574	1084	652	432
	0.993	6.4	2000	1424	1043	381	1578	1015	639	376
	1.987	5.6	2000	1200	893	307	1650	861	556	305
	5.962	4.2	2000	1112	926	186	1709	829	649	180
	9.936	3.9	2000	1081	976	105	1741	825	722	103
2,0	0.199	8.7	2000	1589	1001	588	1895	1496	909	587
	0.396	7.7	2000	1496	900	596	1894	1405	810	595
	0.596	7.1	2000	1488	940	548	1897	1393	847	546
	0.993	6.4	2000	1354	841	513	1894	1259	746	513
	1.987	5.4	2000	1298	812	486	1901	1218	733	485
	5.962	4.0	2000	1242	895	347	1892	1158	815	343
	9.936	4.1	2000	1034	814	220	1903	963	746	217
1,1	0.199	9.0	2000	1564	1024	540	1797	1366	829	537
	0.396	8.2	2000	1405	932	473	1816	1230	758	472
	0.596	7.2	2000	1497	993	504	1785	1288	791	497
	0.993	6.6	2000	1318	893	425	1813	1138	721	417
	1.987	5.9	2000	1071	752	319	1817	900	583	317
	5.962	4.4	2000	1078	854	224	1844	927	706	221
	9.936	4.0	2000	1071	923	148	1831	915	767	148

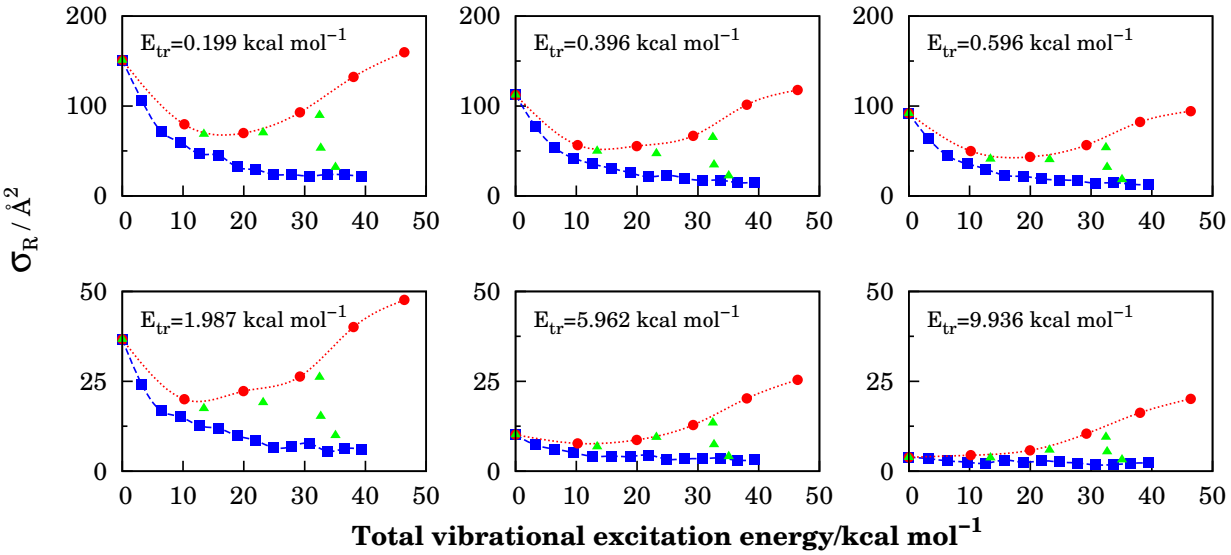

Fig. 3 Reactive cross section for different initial conditions with one and both reactants vibrationally excited. The circles (red), squares (blue) and triangles (green), show, respectively, the theoretical results when vibrational energy is deposited in OH, SO and both reactants.

are vibrationally excited. For five selected combinations, the results showed that the values of the cross section fall between the values obtained with one of the reactants vibrationally excited (see Figure 3) demonstrating that the tendency to increase the cross section with the excitation of the OH radical is compensated by the decreasing action of the excitation of the SO molecule.

In order to understand this behavior it is important to consider which factors favor the formation of the complex and its evolution towards the products. Figure 4 displays, with filled diamonds how the complex formation is influenced by the vibrational excitation. There, little changes are observed in the probability of forming the complex (N_{com}/N_T) as vibrational energy is deposited in either the OH or in the SO species. Thus, according to these results, the formation of the complex is rather independent of the reactants vibrational energy and also independent on which reactant is vibrationally excited. Such relative small variations in the probability of forming the complex are related to changes produced in the multipolar moments of the reactants as they are excited vibrationally. To estimate how much the dipole moments change when the species are vibrationally excited, we used the DMBE PES to calculate them as a function of the respective internuclear distances[15,34,35]. The results are shown in Figures 5(a) and 5(b) together with the classical turning points, in the insets, for several vibrational energies of each reactant. It is clear from Figures 5(a) and 5(b) that the dipole moments of the vibrationally excited species change very little relative to the respective ground state values. Therefore, from the previous analysis we can conclude that most of the influence of the vibrational energy on the reactive cross section, shown in Figure 3, must be related to the evolution of the reaction once the complex is formed. This is also illustrated in Figure 4. Filled circles and triangles represent the reaction probability after the complex was formed (N_R/N_{com}), for vibrationally excited OH and SO species respectively. Notice that the shapes of these plots are very similar to the ones in Figure 3. Again, different behaviors are observed, depending on which of the species is vibrationally excited. Thus, the complex evolution towards the products depends not only on the vibrational energy but also on which reactant is excited. After the complex formation the molecule experiment two competitive processes: reaction and vibrational relaxation. The reaction requires the rupture of the OH bond of the complex, a process that should be favored by the amount of energy in the vibrational mode associated to that bond. On the other hand, to promote the reaction, any amount of vibrational energy initially deposited on the SO species should be quickly transferred to the OH bond. Table 2 shows the values of specific initial-state deactivation probabilities calculated using equation 8 considering all the non reactive trajectories and only the recrossing trajectories for cases in which similar energies are used to vibrationally excite the

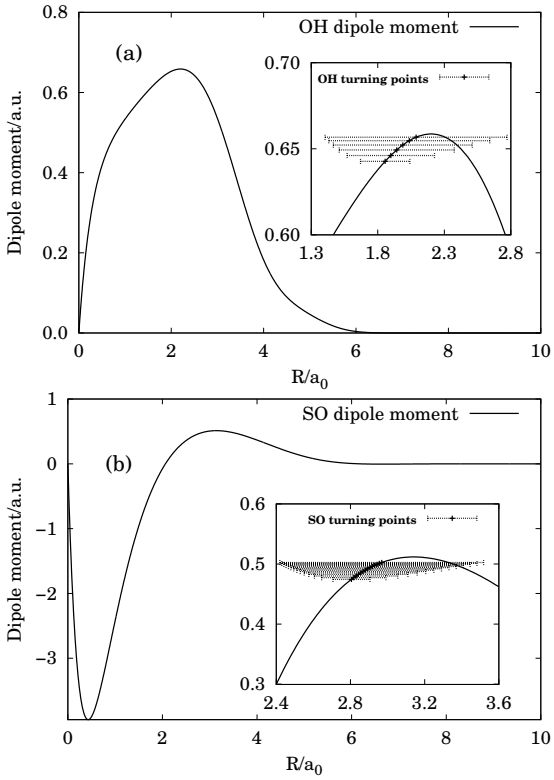

Fig. 5 Dipole moments for OH, panel (a) and SO, panel (b) as a function of diatomic bond length, according to the DMBE PES used in this work. The insets show a zoom in of the same plots and also the classical turning points for the corresponding vibrational level of each species, $v_{OH} = 0-5$, $v_{SO} = 0-14$.

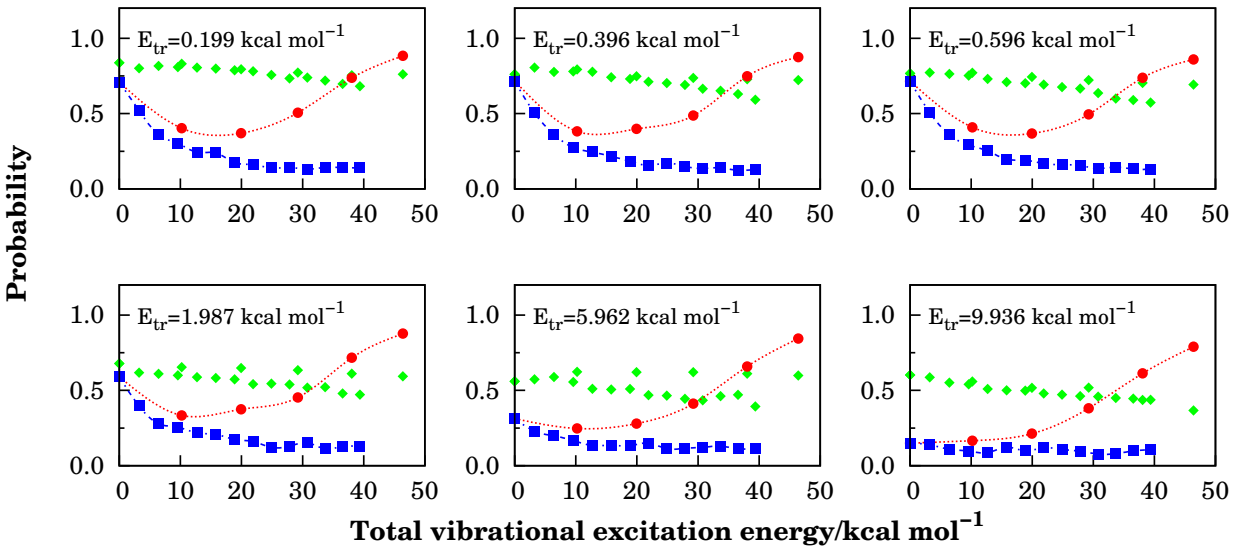

Fig. 4 Probability of forming the complex (N_{com}/N_T) (diamonds, green) as a function of vibrational excitation energy, for selected translational energies. Reaction probability after the complex is formed (N_R/N_{com}) as a function of OH (circles, red) or SO (squares, blue) vibrational excitation energy, for selected translational energies.

Table 2 Deactivation probabilities for selected ro-vibrational combinations of the reactants with similar energies (energies in kcal mol^{-1})

v_{OH}, v_{SO}	E_v^{SO}	E_{tr}	QCT		v_{OH}, v_{SO}	E_v^{OH}	E_{tr}	QCT	
			$P_{rec}^{\downarrow}$	$P_T^{\downarrow}$				$P_{rec}^{\downarrow}$	$P_T^{\downarrow}$
0, 3	9.587	0.199	0.530	0.618	1, 0	10.199	0.199	0.417	0.470
		0.396	0.533	0.619			0.396	0.406	0.459
		0.596	0.504	0.598			0.596	0.398	0.443
		0.993	0.491	0.591			0.993	0.374	0.430
		1.987	0.421	0.565			1.987	0.366	0.425
		5.962	0.405	0.561			5.962	0.367	0.429
		9.936	0.344	0.495			9.936	0.330	0.390
0, 13	39.386	0.199	0.580	0.859	4, 0	38.058	0.199	0.191	0.379
		0.396	0.507	0.798			0.396	0.179	0.350
		0.596	0.496	0.810			0.596	0.184	0.352
		0.993	0.438	0.742			0.993	0.160	0.336
		1.987	0.404	0.740			1.987	0.170	0.387
		5.962	0.329	0.690			5.962	0.203	0.461
		9.936	0.370	0.747			9.936	0.162	0.369

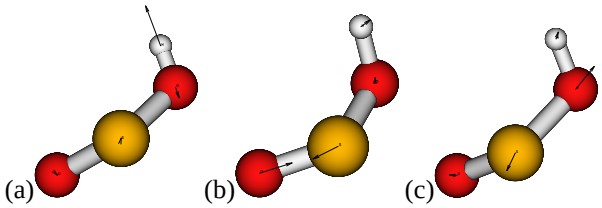

Fig. 6 Vibration modes of the HOSO global minimum, from HSO_2 PES[15]. Panel (a) displays OH stretching $\nu_1 = 3699.52$ cm^{-1}, panels (b) and (c) display SO stretchings $\nu_2 = 1331.64$ cm^{-1} and $\nu_3 = 856.27$ cm^{-1} respectivelly.

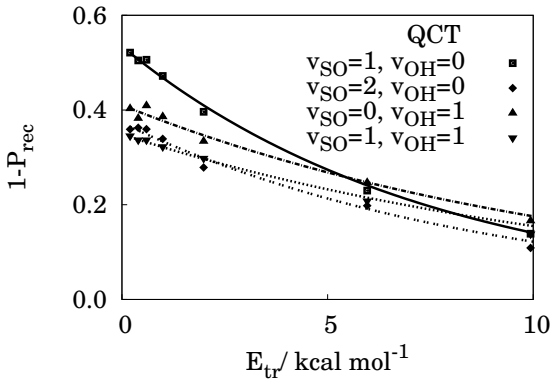

Fig. 7 Probability of reaction after the formation of the complex $(1-P_{rec})$ versus translational energy (E_{tr}) with its respective fitted functions, $P_{rec} = \frac{N_{rec}}{N_{com}}$ is the probability of a trajectory to recross back to reactants after forming a complex. Some selected vibrational combinations are shown.

OH or the SO species. From the results in Table 2 it can be seen that the relaxation processes are more intense when the SO species is excited. Examining the vibration modes of the complex it is possible to identify three modes which are basically associated to stretching of the OH and the two SO bonds, shown in Figure 6.

Assuming that the complex is formed with excess of vibrational energy in the SO bonds, for the reaction to take place it would be required $n(2\nu_2+\nu_3)$ quanta of energy to be internally transferred to the OH bond. However, any increase in the amount of vibrational energy on those modes will also increase the probability of relaxation. On the other hand, the transfer of energy from the OH bond to the SO bonds would required multiple excitations of those bonds, a process less probable than the single-bond rupture.

4.1 Reaction rate constant

As the title reaction is a barrier-less process (Figure 1), the reactive cross section can be also expressed as:

$$\sigma_R(E_{tr};E_{vib};E_{rot}) = n\pi(n-2)^{(2-n)/n}\times \\ \times\left(\frac{C_n}{2E_{tr}}\right)^{2/n} F_{rec}(E_{tr};E_{vib};E_{rot}) \qquad (9)$$

where the first term represents the capture cross section[32,36] and $F_{rec}(E_{tr};E_{vib},E_{rot})$ accounts for recrossing effects, which depends on the translational, vibrational and rotational energies. It was found convenient to use for F_{rec} the same expression of a previous study[11]:

$$F_{rec} = \exp\left[-\alpha(E_{tr}+E_0)\right] \qquad (10)$$

From such expression (with $\alpha > 0$), the probability of the reaction to take place after the complex is formed, descreases when increasing an effective value of energy $E_{eff} = E_{tr} + E_0$. This energy is given by the sum of the initial translational energy E_{tr} and a certain amount of energy E_0 depending on the internal energy of the reactants. It must be remarked that here and before[11], recrossing effects are considered as a correction to the capture cross section, differently from considering the recrossing factor just in rate constant[32]. In the first case one may have dependence of such a factor on the translational and internal energy of the reactants while the recrossing factor in the rate constant is only a function of the temperature.

Substituting Eq. 9 in Eq. 5 and integrating, one gets:

$$k(T;\nu_{OH},j_{OH},\nu_{SO},j_{SO}) = k_{cap}(T;\nu_{OH},j_{OH},\nu_{SO},j_{SO})\times \\ \times\frac{\exp(-\alpha E_0)}{\left(1+\frac{T}{T_0}\right)^{2(n-1)/n}} \qquad (11)$$

where k_{cap} is given by:

$$k_{cap}(T;\nu_{OH},j_{OH},\nu_{SO},j_{SO}) = 2n\pi g_e(T)(n-2)^{(2-n)/n}\times \\ \times\left(\frac{2}{\pi\mu}\right)^{1/2}(k_BT)^{(n-4)/2n}\times \\ \times\left(\frac{C_n}{2}\right)^{2/n}\Gamma\left[\frac{2(n-1)}{n}\right] \qquad (12)$$

where $T_0 = 1/(\alpha k_B)$ and the parameters α, E_0,n and C_n are obtained by fitting $1-P_{rec}$ x E_{tr} to the function in Eq. 10 and σ_R x E_{tr} to Eq. 9 (see Figure 7). The rotational effects were analyzed using a linear approximation for the coefficients (Table 3) as a function of ro-vibrational energy[11]. To examine the effect of both vibrational and rotational excitations on the average rate constants it was first necessary to choose population distributions. We found appropriate to use Boltzmann distributions for the population of rotational levels of both reactants, as well as for the population of the OH vibration levels. However, to compare our theoretical results with experimental values of the rate constant reported by Blitz *et al.*[14] a non-equilibrium distribution was used, based on the following reasoning. According to the experimental work[14], SO was

Table 3 Coefficients from the fitting of the cross section and recrossing factor to functions in Eq. 9 and Eq. 10 respectively

v_{SO}, j_{SO}	v_{OH}, j_{OH}	QCT				$VEQMT_C$			
		n	C_n	α	E_0^a	n	C_n	α	E_0^a
0,0	0,1	4.328	389.604	0.004	0.149	4.561	944.862	0.101	−0.752
0,60	0,12	4.064	63.903	0.002	0.087	3.464	36.725	0.244	0.091
1,0	0,1	4.032	233.113	0.010	0.134	3.778	130.102	0.111	0.123
1,60	0,12	3.988	56.499	0.001	0.074	4.205	63.178	0.001	0.079
2,0	0,1	4.270	326.124	0.002	0.112	3.795	127.657	0.009	0.114
2,60	0,12	2.765	12.692	0.329	0.056	2.700	10.584	0.349	0.060
3,0	0,1	3.919	185.424	0.009	0.095	4.087	203.660	0.006	0.103
3,60	0,12	4.484	97.703	0.003	0.051	4.395	74.873	0.012	0.052
0,0	1,1	3.987	200.845	0.022	0.085	3.947	174.125	0.057	0.087
0,60	1,12	4.077	59.184	0.187	0.048	4.089	54.428	0.200	0.049
4,0	0,1	4.082	221.932	0.019	0.092	4.013	175.363	0.016	0.097
4,60	0,12	4.124	62.216	0.094	0.044	4.060	50.595	0.124	0.047
1,0	1,1	3.924	185.571	0.045	0.081	3.853	153.124	0.033	0.081
1,60	1,12	3.963	51.153	0.216	0.043	3.940	45.586	0.231	0.044
5,0	0,1	3.548	97.291	0.146	0.064	3.513	84.504	0.149	0.070
5,60	0,12	4.346	80.508	0.004	0.057	4.506	89.866	0.000	0.061

[a] in kcal mol^{-1}.

obtained from the photolysis of Cl_2SO at 193nm[37] and the authors assumed that SO was effectively relaxed before the reaction with OH takes place. To our knowledge, however, there are no reports of SO vibrational relaxation at conditions similar to those used in the experiments. Thus, we find convenient to use the population of vibrational levels of SO as given by the vibrational distribution of the nascent SO obtained from the photolysis of Cl_2SO at 193nm[37]. Thus, we have:

$$P_j(T) = (2j+1)\exp\left(-\frac{\Delta E_j}{k_B T}\right) \quad (13)$$

with

$$E_j = (\beta_j j - \alpha_j j(v+\frac{1}{2}))(j+1) \quad (14)$$

for the population of rotational levels of both reactants,

$$P_{v_{OH}}(T) = \exp\left(-\frac{\hbar\omega v_{OH}}{k_B T}\right), \quad (15)$$

for the distribution of vibrational levels of OH, and

$$P_{v_{SO}}(T) = A\exp\left(-\frac{(E_{v_{SO}} - B)^2}{C^2}\right), \quad (16)$$

for the vibrational populations of SO. In the above equations, β_j and α_j are, respectively, the rotational constant and the vibration-rotation coupling constant for the reactants, A, B and C are coefficients obtained from the fitting of the experimental distribution[37] to a Gaussian function (see Figure 8). Finally, the average rate constant is then given by:

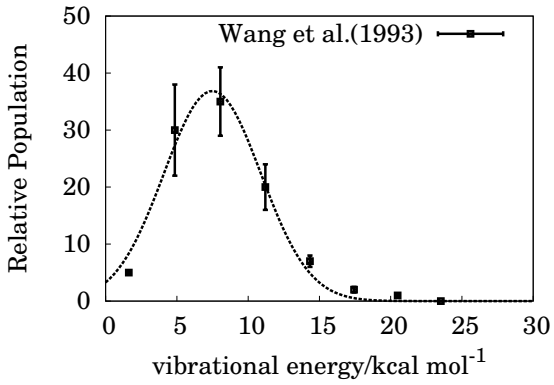

Fig. 8 Vibrational state distribution of the nascent SO fragment following the photolysis of Cl_2SO at 193 *nm* is presented combined with its fit of the Gaussian function, relative the vibrational energy.

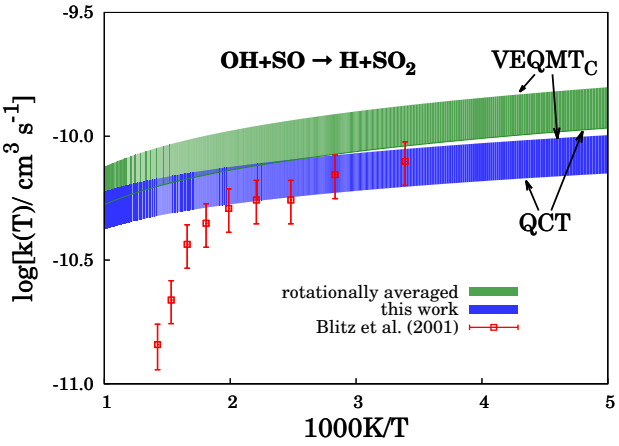

Fig. 9 Rate constant for the title reaction. The theoretical results obtained in this work are given by the region (blue) limited by QCT (bottom curve) and VEQMT$_C$ (upper curve) methods. For comparison, rate constant from rotationally averaged calculation presented in Ref. 11 are also displayed (green). Experimental data are presented with the respective error bars.

$$\langle k \rangle = \sum_{v_{OH}=0}^{2} \sum_{v_{SO}=0}^{6} \sum_{j_{OH}=1}^{12} \sum_{j_{SO}=0}^{60} DP_{v_{OH}} P_{v_{SO}} P_{j_{OH}} P_{j_{SO}}(T) \times \\ \times k(T; v_{OH}, j_{OH}, v_{SO}, j_{SO}), \quad (17)$$

where D is a normalization constant, such that:

$$\sum_{v_{OH}=0}^{2} \sum_{v_{SO}=0}^{6} \sum_{j_{OH}=1}^{12} \sum_{j_{SO}=0}^{60} DP_{v_{OH}} P_{v_{SO}} P_{j_{OH}} P_{j_{SO}}(T) = 1 \quad (18)$$

Figure 9 shows a comparison of the average rate constants reported in the literature and the values obtained with both the QCT and VEQMT$_C$ methods, together with the results previously obtained considering only the rotational excitation of the reactants. The VEQMT$_C$ results represent an upper limit for the predicted rate constants while the lower limit is provided by the QCT results. From Figure 9 it is clear that a better agreement is found between the theory and experiments when ro-vibrational excitation of the reagents are considered than when only rotational excitations were considered[11]. However, from both Figure 9 and Table 4 it is clear that disagreement still persists for temperatures above 550K. Considering that neither in this work nor in the reviewed literature a proper justification of the sudden fall in the rate constant of the title reaction for higher temperature is presented, further experimental and theoretical studies are required as pointed by Blitz *et al*[14].

5 Conclusions

Quasi-classical trajectory methods have been used to study the role of reactant's ro-vibrational energy on the OH + SO collision, and the results obtained clearly indicate the need to take into account both rotational and vibrational degrees of excitations of the species, besides the translation energy, in order to properly describe the reaction. The reactive cross section depends differently on the vibrational energy of the reactants. It decreases when the OH radical is vibrational excited to $v_{OH} = 1$, and then rises with a further increase of vibrational energy, while only a decrease of the cross section is observed when the SO molecule is the excited species. This behavior is explained considering both the probability of forming the complex and the reaction probability once complex is formed. It was verified that the probability of forming the complex is rather independent of the vibrational excitation, regardless of the reactant being excited, but depends on the relative translational energy. However, the probability of dissociation of the complex towards the products significantly depends upon the vibration energy and also on which reactant was vibrationally excited, showing the same behavior as the reactive cross section. The average rate constant was calculated by fitting the reactive cross section to a capture-like model jointly with a factor that takes recrossing effects into account. The results obtained for the rate coefficient agree well with the experimental data below 550 K, but show large discrepancy for higher temperatures.

Table 4 Rate constant (in 10^{-11} cm^3 s^{-1}) for the OH + SO reaction. Experimental results are from the work of Blitz *et al.*[14] except when indicated

T/K	$\langle k(v_{OH}, j_{OH}, v_{SO}, j_{SO}) \rangle$	experiment
295	6.24 – 8.89	7.91 ± 1.58
298	6.22 – 8.86	11.6 ± 5.0^a
300	6.21 – 8.84	8.4 ± 1.5^b
353	5.90 – 8.40	7.00 ± 1.40
403	5.67 – 8.05	5.53 ± 1.10
453	5.47 – 7.76	5.53 ± 1.10
503	5.30 – 7.52	5.11 ± 1.02
553	5.14 – 7.30	4.45 ± 0.89
603	5.00 – 7.10	3.66 ± 0.73
653	4.88 – 6.92	2.18 ± 0.43
703	4.76 – 6.76	1.44 ± 0.30

[a] from Ref. 12
[b] from Ref. 13

Acknowledgments

The authors acknowledge FAPEMIG (CEX APQ 00895/11), FAPERJ and CNPq (Projeto Pró-Sul 490252/2011-7) for financial support. Computational facilities from LCAD of the UNILA are also appreciated. WADP thanks PROPESQ/UFJF for the research grant (BIC).

References

1 R. P. Wayne, *Chemistry of Atmospheres*, Oxford University Press, 2002.
2 P. Glarborg, D. Kubel, K. Dam-Johansen, H.-M. Chiang and J. W. Bozzelli, *Int. J. Chem. Kinet.*, 1996, **28**, 773.
3 J. W. E. Wilson, *Phys. Chem. Ref. Data.*, 1972, **1**, 535.
4 K. Schofield, *J. Phys. Chem. Ref. Data*., 1973, **2**, 25.
5 T. Stoecklin, C. E. Dateo and D. C. Clary, *J. Chem. Soc. Faraday Trans.*, 1991, **87**, 1667.
6 D. C. Clary, T. S. Stoecklin and A. G. Wickham, *J. Chem. Soc. Faraday Trans.*, 1993, **89**, 2185.
7 A. J. Frank, M. Sadílek, J. G. Ferrier and F. Tureček, *J. Am. Chem. Soc*., 1997, **119**, 12343.
8 M. U. Alzueta, R. Bilbao and P. Glarborg, *Combust. Flame*, 2001, **127**, 2234.
9 S. P. Sander, R. R. Friedl, D. M. Golden, M. J. Kurylo, G. K. Moorgat, P. H. Wine, A. R. Ravishankara, C. E. Kolb, M. J. Molina, B. J. Finlayson-Pitts, R. E. Huie and V. L. Orkin, *Chemical kinetics and photochemical data for use in atmospheric modeling.*, Jet propulsion laboratory, nasa technical report, 2006.
10 M. Y. Ballester and A. J. C. Varandas, *Chem. Phys. Lett.*, 2007, **433**, 279.
11 M. Y. Ballester, Y. Orozco-Gonzalez, J. de Dios Garrido and H. F. dos Santos, *J. Chem. Phys.*, 2010, **132**, 044310.
12 R. W. Fair and B. A. Thrush, *Trans. Faraday Soc.*, 1969, **65**, 1557.
13 J. L. Jourdain, G. L. Bras and J. Combourieu, *Int. J. Chem Kinet.*, 1979, **11**, 569.
14 M. A. Blitz, K. W. McKee and M. J. Pilling, *Proceedings of the Combustion Institute*, 2000, **28**, 2491.
15 M. Y. Ballester and A. J. C. Varandas, *Phys. Chem. Chem. Phys.*, 2005, **7**, 2305.
16 S. E. Wheeler and H. F. Schaefer III, *J. Phys. Chem. A*, 2009, **113**, 6779.
17 M. Y. Ballester, P. J. S. B. Caridade and A. J. C. Varandas, *Chem. Phys. Lett.*, 2007, **439**, 301.
18 M. C. McCarthy, V. Lattanzi, O. Martinez Jr., J. Gauss and S. Thorwirth, *J. Phys. Chem. Lett.*, 2013, **4**, 4074.
19 J. D. Garrido, M. Y. Ballester, Y. Orozco-Gonzalez and S. Canuto, *J. Phys. Chem. A*, 2011, **115**, 1453.
20 G. N. Freitas, J. D. Garrido, M. Y. Ballester and M. A. Chaer Nascimento, *J. Phys. Chem. A*, 2012, **116**, 7677–7685.
21 W. L. Hase, *MERCURY: a general Monte-Carlo classical trajectory computer program, QCPE#453. An updated version of this code is VENUS96: W. L. Hase, R. J. Duchovic, X. Hu, A. Komornik, K. F. Lim, D.-H. Lu, G. H. Peslherbe, K. N. Swamy, S. R. van de Linde, A. J. C. Varandas, H. Wang, R. J. Wolf, QCPE Bull 1996,* 16, *43*.
22 A. J. C. Varandas, *J. Chem. Phys.*, 1993, **99**, 1076.
23 M. Karplus, R. Porter and R. D. Sharma, *J. Chem. Phys.*, 1965, **43**, 3259.
24 D. G. Truhlar, *J. Chem. Phys.*, 1972, **56**, 3189.
25 J. T. Muckerman and M. D. Newton, *J. Chem. Phys.*, 1972, **56**, 3191.
26 A. J. C. Varandas, *Int. Rev. Phys. Chem.*, 2000, **19**, 199.
27 L. Bonnet and J. Rayez, *Chemical Physics Letters*, 1997, **277**, 183 – 190.
28 W. Arbelo-González, L. Bonnet, P. Larrégaray, J.-C. Rayez and J. Rubayo-Soneira, *Chemical Physics*, 2012, **399**, 117.
29 A. J. C. Varandas and L. Zhang, *Chem. Phys. Lett.*, 2001, **340**, 62.
30 A. J. C. Varandas, *Chem. Phys.*, 1982, **69**, 295.
31 J. D. Garrido, P. J. S. B. Caridade and A. J. C. Varandas, *J. Phys. Chem. A*, 2002, **106**, 5314.
32 A. J. C. Varandas, Conferencias Plenarias de la XXIII Reunión bienal de Química, Universidad de Salamanca, 1991, p. 321.
33 M. Brouard, *Reaction Dynamics*, Oxford Unversity Press, 1998.
34 J. A. Sabín, S. P. J. Rodrigues and A. J. C. Varandas, *J. Phys. Chem. A*, 2002, **106**, 556.
35 E. Martínez-Núñez and A. J. C. Varandas, *J. Phys. Chem. A*, 2001, **105**, 5923.
36 M. T. Bell and T. P. Softley, *Mol. Phys.*, 2009, **107**, 99.
37 X. C. Hongxin Wang and B. R. Weiner, *J. Phys. Chem.*, 1993, **97**, 12260.

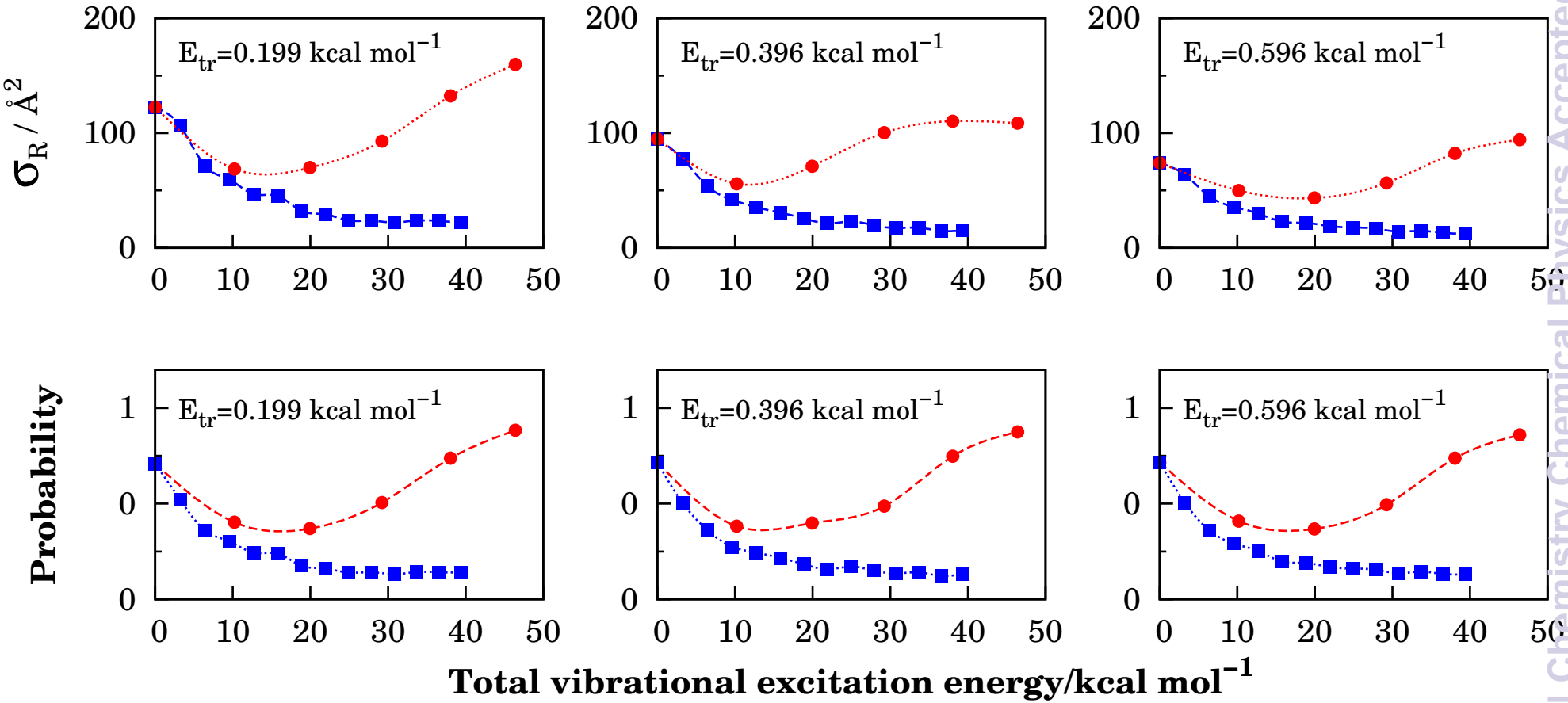

Reaction cross section and reaction probability after forming the complex as a function of reactants vibrational energy.